This article has been accepted for publication in a future issue of this journal, but has not been fully edited. Content may change prior to final publication. Citation information: DOI 10.1109/TNB.2021.3065725, IEEE Transactions on NanoBioscience

Biosensor based on In_2O_3 Electrolyte Gated Thin Film Transistor with Integrated On-Chip Gate Electrode

Peng Yang, Haofeng Rong, Zhisheng Wu, and Yanli Pei

***Abstract*—In this work, In_2O_3 electrolyte gated thin film transistors (In_2O_3-EGTFTs) with integrated on-chip gate electrode were investigated as a label-free biosensor. The In_2O_3 channel works as sensitive membrane and the on-chip gate electrode replaces reference electrode. The pH sensitivity of the device is 64 mV/pH with the deviation of 10 mV. The In_2O_3 channel was coated by streptavidin/neutravidin receptors to detect the target biomolecules of biotin. The streptavidin modified device presents an ultra-low working voltage (V_G=0 V, V_{DS}=50 mV) and the detection limit as low as 50 pg·mL^{-1}. And the neutravidin modified device presents apparent detecting performance even in low biotin concentration of 50 fg·mL^{-1} under a working voltage of V_G=2 V and V_{DS}=50 mV. This work provides a high-performance biosensor device with low power consumption and simple structure that is easy to integrate and package.**

***Index Terms*—On-chip gate, In_2O_3 TFT, electrolyte, biosensor.**

I. Introduction

BIOSENSORS based on indium oxide (In_2O_3) thin film transistors (TFTs) have been widely studied. It shows good biological compatibility, fast response for real-time, high uniformity, and large detectable concentration range [1]-[6]. In addition, the exposed In_2O_3 channel region can be easily modified by various functional groups or receptors, making In_2O_3 biosensor suitable for a variety of biosensors, such as uric acid, dopamine, glucose, cancer antigen 125 (CA-125) and insulin-like growth factor II, etc [3]-[6]. In previous work, we have prepared a high sensitivity pH sensor based on In_2O_3 electrolyte gated TFTs (EGTFTs) and applied as biosensor. The sensitivity of 150 nA·dec^{-1} and detection limit of 50 ng·mL^{-1} were obtained for biotin detection through specific linkage with streptavidin [11]. The result is important for development of biosensing technology. In general, pH detection is valued as the core of biosensing technology. A lot of biological processes or molecules can be detected indirectly by pH change, for example, the processes of DNA sequencing and glucose oxidation [7], [8]. Furthermore, as a typical specific biological binding pair, avidin-biotin pair has been widely used to detect bio-molecules such as atrazine and urea by bio-molecules biotinylation [9], [10]. Considering the possibility of biotinylation of numerous bio-molecules, the research of sensing technology for the specific binding of avidin-biotin is expected to greatly promote the development of biosensing technology. However, in that work, a gold tip was used as an external gate electrode, and immersed in phosphate buffer solution (PBS), directly. The integration and package of the device will be big problems for further practical application. Also, the detection limit needs to improve further.

In order to improve the integration and the packability of the device, we developed an integrated on-chip gate electrode biosensor based on the In_2O_3 EGTFT, which replaced the external gold tip gate electrode. The electric double layer (EDL) serves as gate dielectric in EGTFTs. The integrated plane electrode on chip can modulate the channel electronic characteristics through EDL just like reference electrode. The pH and biotin detection properties were investigated using this integrated on-chip gate electrode biosensor device.

II. Experimental

In_2O_3-EGTFT based biosensors with an integrated on-chip gate electrode were fabricated using conventional semiconductor microfabrication techniques. Firstly, a 15 nm-thick In_2O_3 thin film was grown on Si/SiO_2 substrate by metal organic chemical vapor deposition (MOCVD) as described in literature [12]. Then, the In_2O_3 channel layer was patterned with a channel width (W) of 1600 μm and a channel length (L) of 400 μm by wet etching process. Secondly, the stack layer of Ti (10 nm)/Au (90 nm) was deposited by electron beam (EB) evaporation and patterned by lift-off process as

This work was supported in part by the Natural Science Foundation of China under Grant 61774172, the Science and Technology Project of Guangdong Province, China, under Grant 2019B010132002, the Natural Science Foundation of Guangdong Province, China, under Grant 2017A030310465, the Science and Technology Planning Project of Guangzhou, China, under Grant 201607020036, GDHVPS (2016), the Basic Research Plan Program of Shenzhen City in 2016 (JCYJ20160509100737182), and the fundamental research funds for the centered universities, under grant 19lgpy81; The work was also supported by Pengcheng Scholar funding of Shenzhen (2018). *(Corresponding author: Yanli Pei)*

Peng Yang, Haofeng Rong, and Zhisheng Wu are with State Key Lab of Optoelectronics Materials & Technologies, School of Electronics and Information Technology, Sun Yat-Sen University, Guangzhou 510006, People's Republic of China (e-mail: yangp68@mail2.sysu.edu.cn; ronghf@mail2.sysu.edu.cn; wuzhish@mail.sysu.edu.cn). Peng Yang and Haofeng Rong contributes equally to this work.

Yanli Pei is with State Key Lab of Optoelectronics Materials & Technologies, School of Electronics and Information Technology, Sun Yat-Sen University, Guangzhou 510006, P. R. China and Department of Electronic Communication and Technology, Shenzhen Institute of Information Technology, Shenzhen, 518172, P.R. China (e-mail: peiyanli@mail.sysu.edu.cn).

This article has been accepted for publication in a future issue of this journal, but has not been fully edited. Content may change prior to final publication. Citation information: DOI 10.1109/TNB.2021.3065725, IEEE Transactions on NanoBioscience

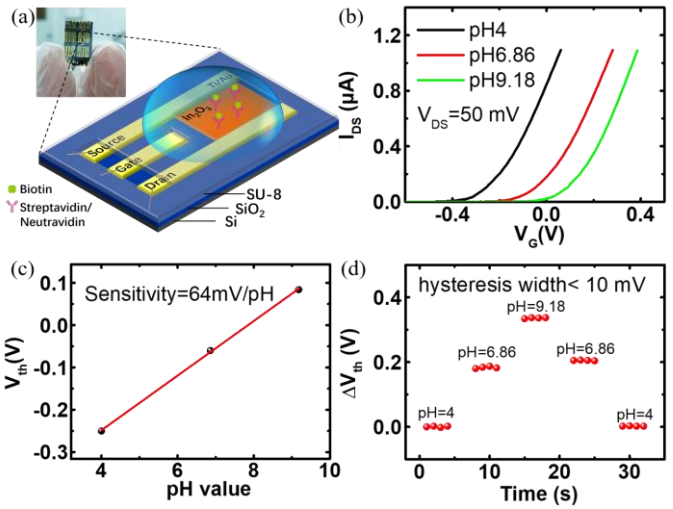

Fig. 1. (a) Schematic diagram and physical image of the In_2O_3-TFT biosensor. (b) The transfer curves of the electrolyte-gated In_2O_3 TFT biosensor measured with various pH buffer solutions from pH 4.00 to pH 9.18. (c) Linear fitting of the Vth as function of the pH value. (d) Time dependent sensing characteristics of the on-chip gated In_2O_3-TFT biosensor.

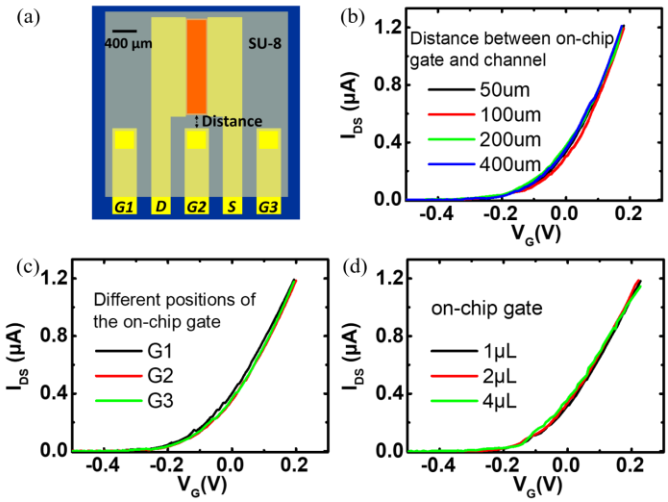

Fig. 2. (a) Schematic diagram of In_2O_3-TFT with different plane gate electrodes. (b) Transfer characteristics of the on-chip gate TFT with different gate-to-channel distances under V_{DS}=0.05V. (c) The transfer characteristics with gate positions of G1, G2 and G3 from left to right respectively. (d) The transfer curve of the In_2O_3 TFT sensor at V_{DS} = 0.05V, pH buffer acting as electrolyte (pH=6.86), and capacity changing from 1 μL to 4 μL.

source, drain (S/D) and on-chip gate (G) electrodes. Finally, the electrodes were passivated with SU-8 polymer to prevent short circuit between S/D through liquid electrolyte solution. The schematic structure and physical image of the In_2O_3-EGTFT sensor are shown in Fig. 1(a). The electrical characteristics are recorded by an Agilent B1500A Semiconductor Parametric Analyzer at room temperature. After one test step, the device was rinsed with DI water and dried with N_2 for next test.

III. Results and Discussion

A. pH Detection

For pH detection, pH buffer solution as liquid gate electrolyte was dripped on the In_2O_3 channel and connected with the on-chip gate electrode. Fig. 1(b) shows the transfer curves of the In_2O_3 EGTFT sensor measured at V_{DS} = 0.05V with various pH buffer solutions from pH 4.00 to pH 9.18. The transfer curves shift to negative direction in parallel with the decrease of the pH value, indicating the increase of the positive potential on the electrolyte/In_2O_3 interface. The result is in good agreement with literature we have reported [13]. Through linear fitting of the V_{th} as function of the pH value, the pH sensitivity of ~64 mV·pH^{-1} with linearity of 98.1% was obtained as shown in Fig. 1(c). Here, the V_{th} was estimated by linear extrapolation method. We noticed that the obtained pH sensitivity is lower than the value of 75 mV·pH^{-1} reported in our previous work [13], where the gold tip is used as external gate electrode. The pH sensitivity may be affected by the fabrication process, especially the evaporation process of gold for on-chip gate electrode.

In order to evaluate the long-term chemical stability of the In_2O_3 EGTFT sensor, the repeated test was demonstrated. As shown in Fig. 1(d), the four measurements at the same pH value show similar V_{th}, indicating that the device has good retention stability. At the same time, the hysteresis width was also measured. It is defined as the difference in V_{th} between the starting pH 4 solution and the final pH 4 solution in a pH measurement loop (pH 4 → pH 6.86 → pH 9.18 → pH 6.86 → pH 4). The hysteresis width was estimated from Figure 1d to be about 10 mV. The long-term chemical stability is significantly improved compared with the V_{th} deviation of 40 mV reported previously [13].

In order to investigate the influence of the gate electrode structure, such as the distance and position of the integrated on-chip electrode to channel, we designed the In_2O_3 EGTFT with different on-chip gate electrodes as showed in the schematic diagram (Fig. 2(a)). Figure 2(b) shows the transfer curves measured from the devices with various gate electrode distances to channel. The curves show negligible difference at the distance range of 50-400 μm. The result is consistent with the characteristics of the electric double layer (EDL) transistor. The device functions through the construction of the EDL at the electrolyte-sensitive layer interface. The capacitance of the EDL is independent on the gate-channel distance varying in a certain range. Integrated on-chip gate electrode utilizes the transverse coupling effect of the electrolyte gate. Also, the position of the on-chip electrode has no significant influence on the device properties. The result shows in Fig. 2(c). These results suggest that the device can operate with multi-gates.

The influence of the electrolyte solution volume on the device properties was investigated. Here, the pH 6.86 buffer solution was used as electrolyte. As shown in Fig. 2(d), the transfer curves are stable even the electrolyte volume is as low as 1μL. The result indicates that with the further reduction of the device size, it is possible to test the submicron pH solution. In contrast, for the device with external gold tip gate electrode, at least 4 μL pH solution is necessary. The good robustness of

This article has been accepted for publication in a future issue of this journal, but has not been fully edited. Content may change prior to final publication. Citation information: DOI 10.1109/TNB.2021.3065725, IEEE Transactions on NanoBioscience

the integrated on-chip gate electrode may be the reason for the improvement of the V_{th} deviation.

B. Electrical Performance of In_2O_3 EGTFT Biosensor

Prior to biological modification, the device was characterized with electrolyte gate of 4μL PBS. The PBS solution is 100 times dilution (0.01M PBS pH 7.4). The transfer curves of the device are showed in Fig. 3(a). We found that the three consecutive tests are essentially identical, indicating the good stability of the device in PBS. V_{th} of -0.13V, I_{on}/I_{off} of ~10^4 are confirmed.

For biotin detection, the streptavidin biomolecules (600 μg·mL^{-1} in 0.1M PBS) and neutravidin (600 μg·mL^{-1} in 0.1M PBS) were immobilized on the aldehyde-functionalized In_2O_3 surface as receptors. It is done by successively coating In_2O_3 active channel surface with ATPES and GA. The immobilized streptavidin and neutravidin molecules have special binding property with biotin. And then, the biotin (N-hydroxysuccinimide ester) (Sigma-Aldrich) in DMF (N, N-Dimethylformamide) was dribbled onto the streptavidin or neutravidin functionalized In_2O_3 surface at room temperature. The detail process was described in literature [11]. Finally, in order to get the biomolecular signals, the 0.01M PBS solution was dripped into the sensing chamber as gate electrolyte, which connected with the integrated on-chip gate electrode. After twice baseline signal establishing in pure 0.01M PBS buffer, we detect the electrical signals of the biotins through monitoring the change of I_{DS}. The concentration of the biotin is from 50 fg·mL^{-1} to 50 μg·mL^{-1} and the interval of each concentration is 10 times. Figure 3(b) shows I_{DS} current versus function of time for streptavidin-biotin linking system. Here, the ultra-low operation voltages of V_G=0V, V_{DS}=50 mV were applied. The arrows indicate the time of the biotin addition. As shown in Fig. 3(b), the current is increased step by step with the increase of the biotin concentration. The result indicates that the biotin as target is captured by the streptavidin. It generates positive potential at the In_2O_3 channel surface.

Figure 3(c) shows ΔI_{DS} as a function of the biotin concentration for the streptavidin modified device. The ΔI_{DS} is defined as I-I_0, where I is the drain current tested at V_G=0 V, V_{DS}=50 mV for the cases with various biotin concentrations, I_0 is the drain current for the case without biotin. The error bar was obtained from device to device fluctuation. We found that the ΔI_{DS} keeps good linearity of 98.4% when the biotin concentration is between 50 pg·mL^{-1} and 5 μg·mL^{-1}. The sensitivity about 280 nA·dec^{-1} was obtained. When the concentration of the biotin was increased to 50 pg·mL^{-1}, the I_{DS} with 100 nA increase was observed. It indicates that the detection limit of the biosensor is as low as 50 pg·mL^{-1}.

Compared with our previous work [11], the detection limit is reduced by three orders of magnitude. It is presumably due to the excellent stability of the In_2O_3 EGTFT with integrated on-chip gate electrode.

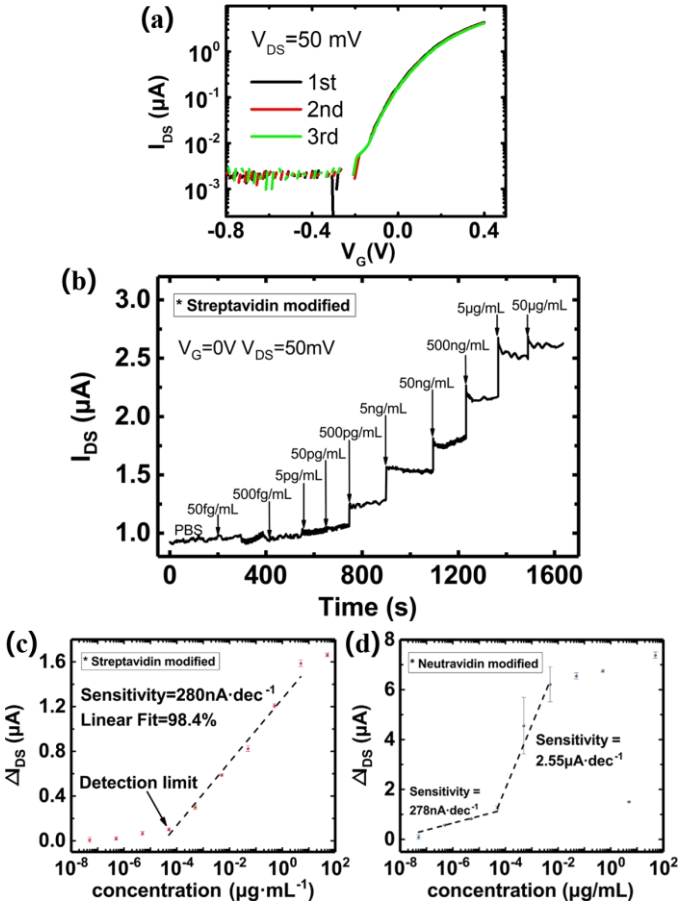

Fig. 3. (a) Transfer characteristics of PBS buffer as electrolyte gate. (b) Current versus time for the streptavidin modified In_2O_3 surface following the addition of biotin solution. (c) Linear fitting of ΔI_{DS} with the change of biotin concentration for the streptavidin modified device. (d) Linear fitting of ΔI_{DS} with the change of biotin concentration for the neutravidin modified device.

However, the increase of ΔI_{DS} is observed to slow down with biotin of concentration larger than 5 μg·mL^{-1}. It indicates that the change of I_{DS}, in other word, the change of the surface potential, tends to saturation. The detectable biotin is limited by the receptors' concentration on the surface of the active layer. When all the streptavidin biomolecules are bound with biotin, theoretically the surface potential and I_{DS} are not able to change any longer.

Furthermore, we have detected the biotin using the neutravidin instead of the streptavidin, with the same method. Differently, the devices with neutravidin modification are tested under a constant gate bias of 2V. Under the conditions of 0 V gate bias, the devices are tested to be in off state. It is presumably due to the different properties in pH value for streptavidin and neutravidin (the former is slightly acidic, while the latter is close to neutral). The result is shown in figure 3(d).

Excitingly, we find that the devices modified by neutravidin show apparent detecting performance even in low biotin concentration of 50 fg·mL^{-1}, and there is no obvious detection

TABLE I
COMPARISON OF SOME BIOSENSORS BASED ON DIFFERENT STRUCTURES

Channel	Target species	Operating Voltage(V)	Sensitivity ($nA \cdot dec^{-1}$)	Detection limit (M)	ref
ZnO nanowire	Streptavidin	<1	20	2.5×10^{-9}	[14]
In_2O_3 nanowire	Cancer antigen	<0.6	10	5×10^{-13}	[4]
Organic P3HT	Biotin	<20	50	1×10^{-11}	[15]
ITO-TFT	Virus H5N1	<1	150	1.5×10^{-7}	[16]
IGZO-TFT	Biotin	<10	220	15×10^{-5}	[17]
In_2O_3-TFT	Dopamine	<10	5	1×10^{-10}	[3]
In_2O_3-TFT(streptavidin)	Biotin	<0.4	280	1.5×10^{-10}	present
In_2O_3-TFT(neutravidin)	Biotin	2	286	1.5×10^{-13}	present

limit in the concentration range where the experiment is conducted. The sensitivity of the devices at the biotin concentration range of 50 $fg \cdot mL^{-1}$ to 50 $pg \cdot mL^{-1}$ is found to be 278 $nA \cdot dec^{-1}$, which is comparable to the sensitivity of the devices modified by streptavidin. However, with the further increase of the biotin concentration, the ΔI_{DS} of the devices increases sharply, while the reproducibility of the devices deteriorates. The sensitivity of the devices is roughly estimated to be 2.55 $\mu A \cdot dec^{-1}$ for biotin concentration ranging from 5 $ng \cdot mL^{-1}$ to 500 $ng \cdot mL^{-1}$. We have not fully understood the mechanism why the performance of the devices changes suddenly, while we will explore this phenomenon more detailly in future works. The ΔI_{DS} of the devices tends to saturation with much higher biotin concentration, similar to the performance of the devices modified by streptavidin, which is limited by the receptors' concentration on the surface of the active layer. According to the measurement so far, the devices modified by neutravidin are more competent for detection of relative low biotin concentration, while the streptavidin modified devices are more competent for detection of higher.

We need to remind that we have not achieved the regeneration of the devices having been used for detecting biotin so far. We will put our hand to this problem in the future work.

The device properties were compared with other groups in Table I. Considering three factors (detection limit, operation voltages, and sensitivity), comprehensively, the In_2O_3 EGTFT with an integrated on-chip electrode is a good candidate for biosensor applications.

IV. CONCLUSIONS

In summary, the In_2O_3 EGTFTs with integrated on-chip gate electrode were fabricated. The pH sensitivity of 64 $mV \cdot pH^{-1}$ was obtained, and the hysteresis width of the cycle test was less than 10 mV. After surface modification, the streptavidin molecules were immobilized on the In_2O_3 channel surface as receptor molecules to capture the target molecules of biotin. The positive charges in the biotin causes an increase in the drain current of the In_2O_3 EGTFT. The biotin detection sensitivity is as high as 280 $nA \cdot dec^{-1}$ under low operation voltage (V_G = 0 V, V_{DS} = 50 mV). The detection limit is 50 $pg \cdot mL^{-1}$. Compared with our previous work, the detection limit is reduced by three orders of magnitude. Furthermore, for the devices with neutravidin modification, the biotin detection concentration is as low as 50 $fg \cdot mL^{-1}$. This work provides a progressive way to fabricate high performance TFT based biosensor chip.

REFERENCES

[1] Q. Z. Liu, N. Aroonyadet, Y. Song, X. L. Wang, X. Cao, Y. H. Liu, S. Cong, F. Q. Wu, M. E. Thompson, and C. W. Zhou, "Highly sensitive and quick detection of acute myocardial infarction biomarkers using In_2O_3 nanoribbon biosensors fabricated using shadow masks." *ACS Nano,* vol. 10, no. 11, pp. 10117-10125, Nov. 2016. DOI: 0.1021/acsnano.6b05171

[2] Q. Z. Liu, Y. H. Liu, F. Q. Wu, X. Cao, Z. Li, M. Alharbi, A. N. Abbas, M. R. Amer, and C. W. Zhou, "Highly sensitive and wearable In_2O_3 nanoribbon transistor biosensors with integrated on-chip gate for glucose monitoring in body fluids." *ACS Nano,* vol. 12, no. 2, pp. 1170-1178, Feb. 2018. DOI: 10.1021/acsnano.7b06823

[3] J. Kim, Y. S. Rim, H. J. Chen, H. H. Cao, N. Nakatsuka, H. L. Hinton, Z. C. Zhen, A. M. Andrews, Y. Yang, and P. S. Weiss, "Fabrication of high-performance ultrathin In_2O_3 film field-effect transistors and biosensors using chemical lift-off lithography." *ACS Nano*, vol. 9, no. 4, pp. 4572–4582, Oct. 2015. DOI: 10.1021/acsnano.5b01211

[4] H. K. Chang, F. N. Ishikawa, R. Zhang, Ram Datar, R. J. Cote, M. E. Thompson, and C. W. Zhou, "Rapid, label-free, electrical whole blood bioassay based on nanobiosensor systems." *ACS Nano,* vol. 5, no. 12, pp. 9883-9891, Nov. 2011. DOI: 10.1021/nn2035796

[5] N. Aroonyadet, W. Jeamsaksiri, A. Wisitsoraat, and A. Tuantranont, "Top-down and sensitive indium oxide nanoribbon field effect transistor biosensor chips integrated with on-chip gate electrodes toward point of care applications." *Nanotechnology,* vol. 29, no. 40, pp. 405505-405514, Jul. 2018. DOI: 10.1088/1361-6528/aad435

[6] H. J. Chen, Y. S. Rim, I. C. Wang, C. Li, B. Zhu, M. Sun, M. S. Goorsky, X. M. He, and Y. Yang, "Quasi-two-dimensional metal oxide semiconductors based ultrasensitive potentiometric biosensors." *ACS Nano.* vol. 11, no. 5, pp. 4710-4718, May 2017. DOI: 10.1021/acsnano.7b00628

[7] Y. C. Syu, W. E. Hsu, and C.T. Lin, "Review-Field-Effect Transistor Biosensing: Devices and Clinical Applications." *ECS JOURNAL OF SOLID STATE SCIENCE AND TECHNOLOGY*, vol. 7, no. 7, pp. Q3196-Q3207, Jun. 2018. DOI: 10.1149/2.0291807jss

[8] D. S. Juang, C. H. Lin, Y. R. Huo, C. Y. Tang, C. R. Cheng, H. S. Wu, S. F. Huang, A. Kalnitsky, and C. C. Lin, "Proton-ELISA: Electrochemical immunoassay on a dual-gated ISFET array." *BIOSENSORS & BIOELECTRONICS*, vol. 117, pp. 175-182, Oct. 2018. DOI: 10.1016/j.bios.2018.06.012

[9] S. Helali, H.Ben Fredj, K. Cherif, A. Abdelghani, C. Martelet, and N. Jaffrezic-Renault, "Surface plasmon resonance and impedance spectroscopy on gold electrode for biosensor application." *MATERIALS SCIENCE & ENGINEERING: C*, vol. 28, no. 5-6, pp. 588-593, Jul. 2008. DOI: 10.1016/j.msec.2007.10.065

[10] H.Barhoumi, A.Maaref, S.Cosnier, C.Martelet, and N.Jaffrezic-Renault, "Urease immobilization on biotinylated polypyrrole coated ChemFEC devices for urea biosensor development." *IRBM*, vol. 29, no. 2-3, pp. 192-201, Apr.-May 2008. DOI: 10.1016/j.rbmret.2007.11.004

[11] P. Yang, G. Cai, X. Wang, and Y. L. Pei, "Electrolyte-gated indium oxide thin film transistor based biosensor with low operation voltage." *IEEE T. Electron Dev.*, vol. 66, no. 8, pp. 3554-3559, Aug. 2019. DOI: 10.1109/TED.2019.2920990

[12] R. Q. Hu, Y. L. Pei, Z. M. Chen, J. C. Yang, J. Y. Lin, J. Liang, B. F. Fan, and G. Wang, "Correlation between grain orientation and carrier concentration of poly-crystalline In_2O_3 thin film grown by MOCVD." *J. Mater. Sci.*, vol. 50, no. 3, pp. 1058–1064, Feb. 2015. DOI: 10.1007/s10853-014-8662-9

[13] G. S. Cai, L. Qiang, P. Yang, Z. M. Chen, Y. Zhuo, Y. Li, Y. L. Pei, and G. Wang, "High-sensitivity pH sensor based on electrolyte-gated In_2O_3

TFT." *IEEE Electron Device Lett.*, vol. 39, no. 9, pp. 1409–1412, Sept. 2018. DOI: 10.1109/LED.2018.2857925

[14] A. Choi, K. Kim, H. Jung, and S. Y. Lee, "ZnO nanowire biosensors for detection of biomolecular interactions in enhancement mode." *Sens. Actuators B, Chem.*, vol. 117, no. 2, pp. 577-582, May 2010. DOI: 10.1016/j.snb.2010.04.049

[15] E. Macchia, M. Magliulo, K. Manoli, F. Giordano, G. Palazzo, and L. Torsi, "Direct electronic probing of biological complexes formation." *Proc. SPIE*, vol. 9183, pp. 918302-1–918302-10, Oct. 2014. DOI: 10.1117/12.2067934

[16] D. Guo, M. Zhuo, X. Zhang, C. Xu, J. Jiang, F. Gao, Q. Wan, Q. Li, and T. Wang, "Indium-tin-oxide thin film transistor biosensors for label-free detection of avian influenza virus H5N1." *Anal. Chim. Acta,* vol. 773, no. 22, pp. 83–88, Apr. 2013. DOI: 10.1016/j.aca.2013.02.019

[17] T. Y. Chen, T. H. Yang, N. T. Wu, Y. T. Chen, and J. J. Huang, "Transient analysis of streptavidin-biotin complex detection using an IGZO thin film transistor-based biosensor integrated with a microfluidic channel." *Sens. Actuators B, Chem.*, vol. 244, pp. 642–648, Jun. 2017. DOI: 10.1016/j.snb.2017.01.050